16 Neutrino Oscillations

This topic is well covered by Chapter 11 of Griffiths, and there is also a good web site at http://neutrinooscillation.org/.

16.1 Introduction to Neutrinos

Neutrinos are the least understood of the Standard Model fermions. They have zero electric charge and zero colour charge and therefore their only interactions are due to the weak force and gravity. There are known to be exactly three neutrinos with $m_\mu < m_Z/2$.

In the Standard Model neutrinos are described as massless neutral fermions which come in three different flavours, ν_e, ν_μ and ν_τ. Until 1999 the prevailing belief was that neutrinos were, in fact, massless. We now know they have a very small mass, the current limits are $m_\nu < 2$ eV however values for the absolute masses are unknown.

The mass eigenstates of the neutrinos are not identical to the flavour eigenstates. The flavour eigenstates are ν_e, ν_μ, ν_τ; these are the states which are interact with the W and Z boson. The mass eigenstates are labelled ν_1, ν_2 and ν_3 and are linear superpositions of the weak eigenstates; these are the states that propagate through matter and vacua.

The observation of neutrino masses means Standard Model does not correctly describe neutrinos. However for most neutrino phenomena, apart from neutrino mixing, the Standard Model description of neutrinos is sufficient. Neutrino mixing requires a new lepton-flavour violating interaction which is not present in the Standard Model. We do not yet know what this interaction is!

16.2 Description of Oscillations

16.2.1 Two Neutrino Flavours

Neutrinos are produced in weak decays, and therefore they start off as weak eigenstates. However, they propagate through space-time as plane waves corresponding to their mass eigenstates:

$$\nu_1(t) = \nu_1(0)e^{-iE_1 t} \qquad \nu_2(t) = \nu_2(0)e^{-iE_2 t} \tag{16.1}$$

The mixing of two neutrinos can be described in terms of a mixing matrix such as:

$$\begin{pmatrix} \nu_e \\ \nu_\mu \end{pmatrix} = \begin{pmatrix} \cos\theta_{12} & \sin\theta_{12} \\ -\sin\theta_{12} & \cos\theta_{12} \end{pmatrix} \begin{pmatrix} \nu_1 \\ \nu_2 \end{pmatrix} \tag{16.2}$$

where θ_{12} is a new parameter not present in the Standard Model.

If the neutrino masses m_1 and m_2 are different, the energies E_1 and E_2 are different. Assuming highly relativistic neutrinos with $m \ll E$, $p \approx E$:

$$E_i = p + \frac{m_i}{2p^2} \qquad \Delta E = \frac{\Delta m_{12}^2}{E} \tag{16.3}$$

If we start off with a pure ν_e beam, the amplitude for ν_e at a later time t is:

$$\nu_e(t) = \nu_e(0)\left[1 - \sin\theta_{12}\cos\theta_{12}(-e^{-iE_1t} + e^{-iE_2t})\right] \tag{16.4}$$

and the probability of observing an oscillation to ν_μ is:

$$P(\nu_e \to \nu_\mu) = |\nu_\mu(t)|^2 = 1 - |\nu_e(t)|^2 = \sin^2 2\theta_{12}\sin^2\frac{(E_2 - E_1)}{2}t \tag{16.5}$$

For experimental convenience this is usually expressed as:

$$P(\nu_e \to \nu_\mu) = \sin^2 2\theta_{12}\sin^2\left(\frac{1.27\Delta m_{12}^2 L}{E}\right) \tag{16.6}$$

where the numerical factor 1.27 applies if we express Δm^2 in eV^2, the distance from the source L in metres, and the neutrino energy E in MeV.

To observe these oscillations experimentally a "near" detector measures the initial ν_e flux, and a "far" detector measures either disappearance of ν_e, or appearance of ν_μ. The choice of the "baseline", L, has to be matched to the oscillation frequency $1.27\Delta m_{12}^2/E$, and the amplitude of the oscillations is related to the mixing angle by $\sin^2 2\theta_{12}$. *Note that the maximum possible mixing is for* $\theta_{12} = 45°$.

16.2.2 The PMNS Mixing Matrix

For the full case of three neutrinos we have the equivalent of the CKM matrix which is known as the PMNS (Pontecorvo, Maki, Nakagawa, Sakata) matrix. It is usually written out as the product of three matrices representing the three different types of two neutrino mixings:

$$\begin{pmatrix} \nu_e \\ \nu_\mu \\ \nu_\tau \end{pmatrix} = V_{\text{PMNS}} \begin{pmatrix} \nu_1 \\ \nu_2 \\ \nu_3 \end{pmatrix} \tag{16.7}$$

$$V_{\text{PMNS}} = \begin{pmatrix} 1 & 0 & 0 \\ 0 & c_{23} & s_{23} \\ 0 & -s_{23} & c_{23} \end{pmatrix} \begin{pmatrix} c_{13} & 0 & s_{13}e^{i\delta} \\ 0 & 1 & 0 \\ -s_{13}e^{-i\delta} & 0 & c_{13} \end{pmatrix} \begin{pmatrix} c_{12} & s_{12} & 0 \\ -s_{12} & c_{12} & 0 \\ 0 & 0 & 1 \end{pmatrix} \tag{16.8}$$

It is parameterised by three angles, where $s_{ij} = \sin\theta_{ij}$, $c_{ij} = \cos\theta_{ij}$, and one complex phase δ. The observations of neutrino oscillations, described in the next sections, can be accounted for by small mass differences Δm_{12} and Δm_{23}, and large mixing angles θ_{12} and θ_{23}. As in the CKM case, the phase δ can give rise to CP violation in neutrino oscillations, but only if $\theta_{13} \neq 0$.

16.3 Neutrino Experiments

Neutrinos cross sections are very small, therefore any neutrino experiment needs a huge neutrino flux, and a very massive detector, in order to detect a reasonable number of events. There a few man-made and natural sources of neutrino fluxes which can be used:

- Solar Neutrinos: ν_e produced in the sun
- Atmospheric Neutrinos: ν_e, ν_μ from the decay of cosmic rays
- Reactor Neutrinos: $\bar{\nu}_e$ from fusion reactions
- Accelerator Neutrinos: $\nu_\mu, \bar{\nu}_\mu$ from $\pi^\pm$ decays

Different detection techniques are sensitive to different reactions. The main detection mechanisms are W-boson interactions (charged current):

$$\begin{aligned} \nu_e + n \rightarrow p + e^- \quad & \bar{\nu}_e + p \rightarrow n + e^+ \\ \nu_\mu + n \rightarrow p + \mu^- \quad & \bar{\nu}_\mu + p \rightarrow n + \mu^+ \\ \nu_\tau + n \rightarrow p + \tau^- \quad & \bar{\nu}_\tau + p \rightarrow n + \tau^+ \end{aligned} \tag{16.9}$$

and Z-boson interactions (elastic scattering):

$$\nu_e + e^- \rightarrow \nu_e + e^- \quad \nu_\mu + e^- \rightarrow \nu_\mu + e^- \quad \nu_\tau + e^- \rightarrow \nu_\tau + e^- \tag{16.10}$$

16.4 Solar Neutrinos

16.4.1 The Standard Solar Model

The sun creates energy by fusion of light nuclei. During this process a large flux of low energy **electron neutrinos** are released from β^+ decays of the fusion products. Most of the flux comes from the p-p fusion process, in which neutrinos are emitted up to a maximum energy of 400 keV. There is a small component of higher energy neutrinos, up to a maximum of 15 MeV, associated with ^{8}B. A large amount of work, mostly by Bahcall, has gone into calculating the flux of solar neutrinos using a Standard Solar Model (SSM), shown in figure 16.1.

16.4.2 The Davis Experiment

From 1970-1995 Ray Davis looked for solar neutrinos using a large tank containing 100,000 gallons of cleaning fluid placed in a mine in South Dakota. The neutrinos from ^{8}B and ^{7}Be are detected by the interaction:

$$\nu_e + {}^{37}\mathrm{Cl} \rightarrow {}^{37}\mathrm{Ar} + e^- \tag{16.11}$$

As shown in figure 16.2, only 0.5 Argon atoms are produced per day(!). The whole cleaning tank is analysed radiochemically every few months to count these atoms. The observed rate is 2.56 ± 0.23 SNU, whereas predicted rate from the SSM is 7.7 ± 1.2 SNU, resulting in a "solar neutrino deficit" of 0.33 ± 0.06. (One SNU (solar neutrino unit) is 10^{-36} captures per atom per second.)

There was a long discussion about whether the radiochemical extraction of the Argon atoms was reliable, and an equally long discussion about whether the predictions of the

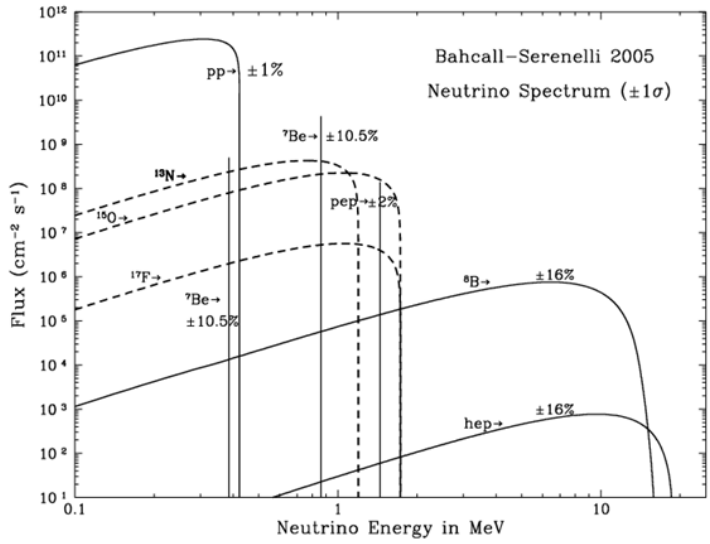

Figure 16.1: Predicted spectrum of solar neutrinos.

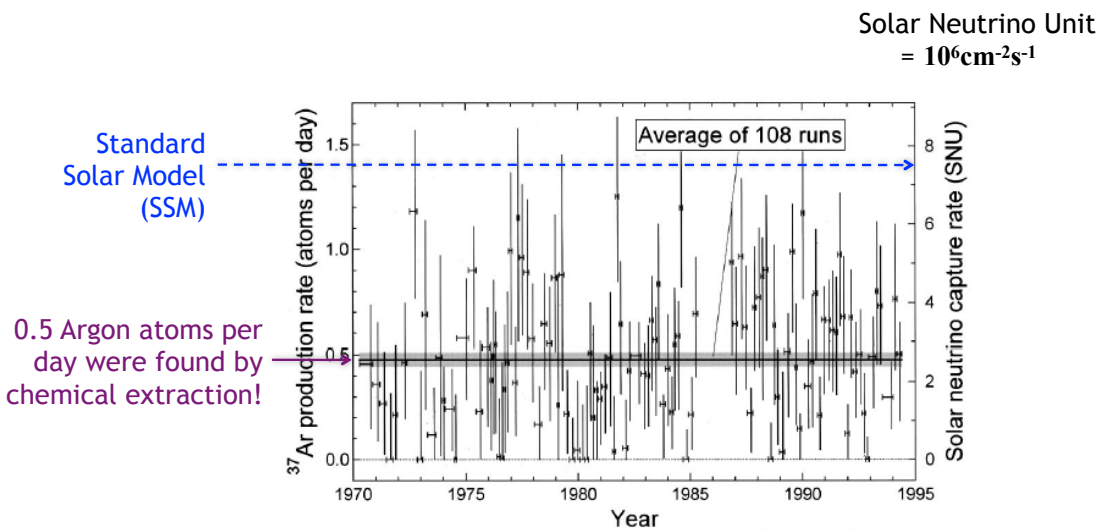

Figure 16.2: Results from the Davis Experiment.

Standard Solar Model were reliable. Now it is accepted that the deficit is real, and is attributable to $\nu_e \to \nu_\mu$ (or ν_τ) oscillations.
Note that due to the low neutrino energy it is impossible to detect ν_μ or ν_τ by charged current interactions.

16.4.3 Recent Solar Neutrino Experiments

The Kamiokande, Gallex and SAGE experiments have also measured solar neutrinos and have also observed a defecit in the number of electron neutrinos.

The SNO experiment proved this between 2000 and 2006 using 1,000 tons of heavy water (D_2O) to detect neutrinos in three different ways:

- Scattering on electrons $\nu_e + e^- \to \nu_e + e^-$
- Charged current scattering on deuterium $\nu_e + d \to p + p + e^-$
- Neutral current scattering on deuterium $\nu + d \to n + p + \nu$

As indicated by the lack of a subscript, the last process does not distinguish between ν_e, ν_μ and ν_τ. The difference between the neutral and charged current scattering on deuterium shows that the ν_μ (or ν_τ) flux is exactly what is required to account for the solar neutrino deficit.

16.5 Propagation of Neutrinos through Matter: The MSW Effect

In 1978 Wolfenstein noted that the effect of flavour-specific neutrino interactions must be taken into account when considering neutrino propagation in the presence of matter. Since matter contains electrons but not muons, electron neutrinos experience a potential energy due to interactions, $U_e \propto G_F N_e$, where N_e is the electron density of the matter. This potential has an equivalent effect to a mass difference, i.e. it changes the energy with which the electron neutrinos propagate. This leads to matter-induced electron neutrino oscillations, with an effective mixing angle in matter θ_m, which differs from θ in vacuum:

$$\sin^2 2\theta_m = \frac{\sin^2 2\theta}{(\cos 2\theta - a)^2 + \sin^2 2\theta} \qquad a \propto G_F E_\nu N_e / \Delta m^2 \tag{16.12}$$

In the sun, the electron density N_e varies with radius, and there can be a radius where $a = \cos 2\theta$ and $\sin^2 2\theta_m = 1$ leads to **resonance-enhanced** oscillations of electron neutrinos. This is known as the MSW effect.

Combining all solar neutrino results, and including the MSW effect, the parameters of the solar neutrino oscillations have been determined to be:

$$\Delta m^2_{12} = (7.6 \pm 0.2) \times 10^{-5} \mathrm{eV}^2 \qquad \sin^2 2\theta_{12} = 0.87 \pm 0.03 \tag{16.13}$$

(There is an alternative solution with vacuum oscillations and no MSW effect. This has a much smaller Δm^2_{12}, but it is ruled out by reactor experiments.)

16.6 Atmospheric Neutrinos

Neutrinos are produced in the upper atmosphere by the interactions of cosmic rays. The initial strong interaction of protons with nuclei produces charged (and neutral) pions. The charged pions decay via $\pi^+ \to \mu^+\nu_\mu$, $\mu^+ \to e^+\nu_e\bar{\nu}_\mu$, and the charge conjugate π^- decays. This gives ratios of two muon (anti)neutrinos to one electron (anti)neutrino. Note that atmospheric neutrinos have much higher energies than solar neutrinos, in the GeV range.

The SuperKamiokande experiment in Japan used 50,000 tonnes of ultra pure water to detect atmospheric neutrinos via the charged current interactions $\nu_e + p \to p + e^-$, $\nu_\mu + p \to p + \mu^-$. The muon and electron can be identified and used to tag the flavour of the incoming neutrino. As illustrated in figure 16.3 what is observed is a deficit of upward going muons, produced by muon neutrinos coming from the atmosphere on the other side of the earth.

This observation is interpreted as the oscillation of muon neutrinos into unobserved tau neutrinos over the earth's diameter, with parameters:

$$\Delta m^2_{23} = (2.4 \pm 0.1) \times 10^{-3}\text{eV}^2 \qquad \sin^2 2\theta_{23} = 1.00 \pm 0.05 \tag{16.14}$$

Note that this mass difference squared is 30 times larger than the solar neutrino mass difference, and that the mixing is consistent with being maximal.

16.7 Accelerator Neutrino Experiments

A typical accelerator neutrino beam is either ν_μ or $\bar{\nu}_\mu$, produced from the decays of $\pi^\pm$ and $K^\pm$ mesons. There is $\sim 1\%$ contamination of ν_e from semileptonic decays. The beam energies are in the range 100 MeV to 10 GeV, and the corresponding baselines range from 1 to 1000 km.

Accelerator beams have been used to confirm the oscillations of $\nu_\mu \to \nu_\tau$. The K2K experiment fired a 1 GeV beam across Japan from KEK to Kamiokande (L =250km). They measured the disappearance of ν_μ, and obtained results consistent with the atmospheric neutrinos. More recently the MINOS experiment fired a 10 GeV beam from Fermilab to Soudan (L =735km), to obtain the world's most accurate values for Δm^2_{23} and $\sin^2 2\theta_{23}$.

Both MINOS and a Japanese experiment, T2K, are now looking for $\nu_\mu \to \nu_e$ appearance to try and measure the small mixing angle θ_{13}.

First results from T2K measure $0.03(0.04) < \sin 2\theta_{13} < 0.28(0.34)$ at 90% confidence level. The two sets of values reflect the different possible orderings of the masses, see figure 16.4.

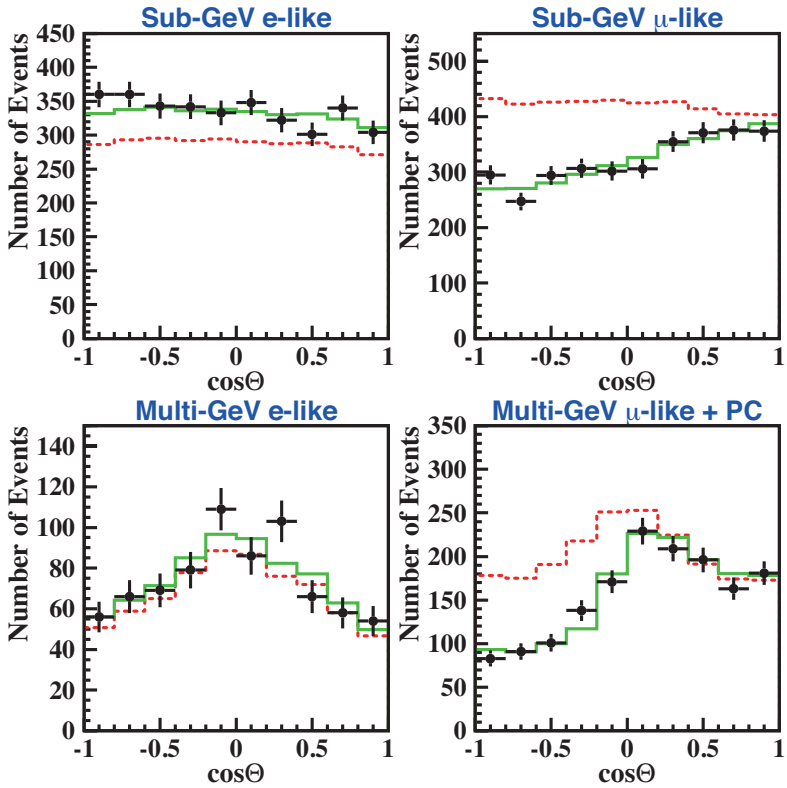

Figure 16.3: The observed (black points) and predicted (lines) number of electron neutrino and muon neutrino events in the SuperKamiokande detector, as a function of the angle of incidence. $\cos\Theta < 1$ corresponds to upwards-travelling neutrinos which have travelled through the earth before arriving in the detector. The red dotted line is the prediction for the number of events, if there was no oscillations of ν_μ. The green line is the fit allowing for neutrino oscillations. The data clearly is more consistent with neutrino oscillations.

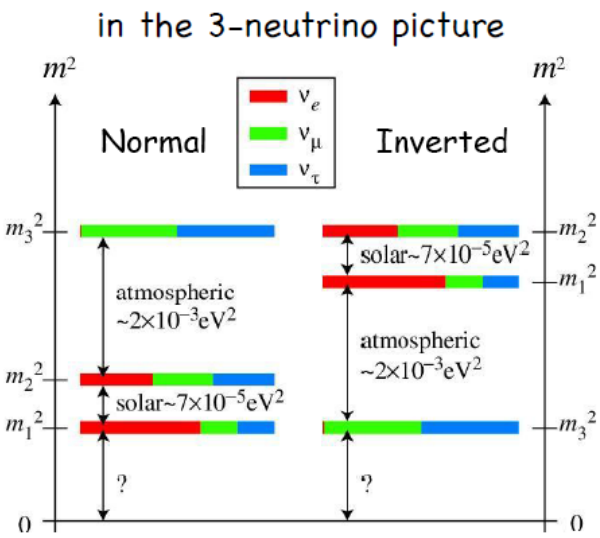

Figure 16.4: Illustration of the masses and composition of the three neutrino mass eigenstates, based on current measurements. There are two possible orderings of the masses.

16.8 Experimental Results

The current results on neutrino masses and mixing are summarised in figure 16.4. The current estimate of the PNMS matrix is:

$$\begin{pmatrix} U_{e1} & U_{e2} & U_{e3} \\ U_{\mu 1} & U_{\mu 2} & U_{\mu 3} \\ U_{\tau 1} & U_{\tau 2} & U_{\tau 3} \end{pmatrix} \sim \begin{pmatrix} 0.85 & 0.53 & 0.1e^{i\delta} \\ -0.37 & 0.60 & 0.71 \\ 0.37 & -0.60 & 0.71 \end{pmatrix} \tag{16.15}$$

Where δ is an unknown CP-violating phase.

However, there are still several open questions about neutrino mixing:

- We do not know the absolute neutrino mass scale. It could be $m \approx \Delta m$, or the masses could be degenerate $m \gg \Delta m$.
- We do not know the mass hierarchy, because we determine the magnitudes but not the signs of the mass differences. It could be "normal" $m_1, m_2 < m_3$, or "inverted" $m_3 < m_2, m_1$. These two possibilities are illustrated in figure 16.4.

16.9 Neutrinos in Astrophysics*

Finally some comments on the role of neutrinos in astrophysics:

- The Big Bang model predicts a large relic density of very low energy neutrinos, similar to the microwave background of photons. However, the mass of neutrinos is too small to account for dark matter.

- In 1987 a few electron neutrinos with E= $10-40$ MeV were observed coming from the Supernova SN1987A in the Large Magellanic Cloud (L =175k light years). The energies and spread of arrival times constrain the neutrino mass, and may eventually provide information on the initial stages of a supernova explosion. We just have to wait for the next one...

- Detectors such as AMANDA at the South Pole, and ANTARES in the Mediterranean detect very high energy neutrinos from outer space. The advantage of neutrinos is that they are unaffected on their path from a point source to the earth.

17 Electroweak Physics

A unified description of the electromagnetic and weak interactions was developed by Weinberg and Salam in 1967. At high energies ($E \gtrsim m_Z$) the electromagnetic force and the weak force are unified as a single electroweak force. At low energies ($E \lesssim m_Z$) the manifestations of the electroweak force are separate weak and electromagnetic forces.

17.1 Weak Isospin and Hypercharge

Analogous to electric charge (for QED) and colour charge (for QCD), **weak isospin** (T, T_3) and **hypercharge** (Y, or weak hypercharge) are the two charges for the electroweak force. Each fermion has a particular value of weak isospin and hypercharge. These two different charges couple to two different (sets of) bosons.

The weak isopsin charge is analogous to spin (and strong isospin) in that it has two components: total weak isospin (T) and the third component of weak isospin (T_3). T_3 can take on values between T and $-T$ in integer steps. The values of T and T_3 for a given fermion depend on the handedness of the fermion (which can be either left or right):

- All left-handed fermions have $T = \frac{1}{2}, T_3 = \pm\frac{1}{2}$.
- All right-handed fermions have zero weak isospin: $T = 0, T_3 = 0$.
- All left-handed antifermions have zero weak isospin: $T = 0, T_3 = 0$.
- All right-handed antifermions have $T = \frac{1}{2}, T_3(\bar{f}) = -T_3(f)$.

Hypercharge (Y) can be defined in terms of the electric charge Q as $Y = 2(Q - T_3)$.

The values for the weak isospin and hypercharge of the fundamental fermions are given in table 1.

The left-handed leptons (i.e. the neutrinos and the left-handed e, μ, τ) form weak isospin doublets, denoted as χ_{L}. All members of the doublets have the same values of T, Y and lepton number L, but are distinguished by different values of T_3. The left-handed quarks also form isospin doublets:

$$\chi_{\mathrm{L}} = \begin{pmatrix} \nu_{e\,\mathrm{L}} \\ e^-_{\mathrm{L}} \end{pmatrix} \begin{pmatrix} \nu_{\mu\,\mathrm{L}} \\ \mu^-_{\mathrm{L}} \end{pmatrix} \begin{pmatrix} \nu_{\tau\,\mathrm{L}} \\ \tau^-_{\mathrm{L}} \end{pmatrix} \quad T = 1/2; \begin{matrix} T_3 = +1/2 \\ T_3 = -1/2 \end{matrix} \tag{17.1}$$

$$\chi_{\mathrm{L}} = \begin{pmatrix} \mathrm{u}_{\mathrm{L}} \\ \mathrm{d}_{\mathrm{L}} \end{pmatrix} \begin{pmatrix} \mathrm{c}_{\mathrm{L}} \\ \mathrm{s}_{\mathrm{L}} \end{pmatrix} \begin{pmatrix} \mathrm{t}_{\mathrm{L}} \\ \mathrm{b}_{\mathrm{L}} \end{pmatrix} \quad T = 1/2; \begin{matrix} T_3 = +1/2 \\ T_3 = -1/2 \end{matrix} \tag{17.2}$$

Lepton	Q	T	I_3	Y	Quark	Q	T	T_3	Y
$\nu_{e\mathrm{L}}, \nu_{\mu\mathrm{L}}, \nu_{\tau\mathrm{L}}$	0	$\frac{1}{2}$	$+\frac{1}{2}$	-1	$\mathrm{u_L}, \mathrm{c_L}, \mathrm{t_L}$	$+\frac{2}{3}$	$\frac{1}{2}$	$+\frac{1}{2}$	$+\frac{1}{3}$
$e_\mathrm{L}, \mu_\mathrm{L}, \tau_\mathrm{L}$	-1	$\frac{1}{2}$	$-\frac{1}{2}$	-1	$\mathrm{d_L}, \mathrm{s_L}, \mathrm{b_L}$	$-\frac{1}{3}$	$\frac{1}{2}$	$-\frac{1}{2}$	$+\frac{1}{3}$
$\nu_{e\mathrm{R}}, \nu_{\mu\mathrm{R}}, \nu_{\tau\mathrm{R}}$	0	0	0	0	$\mathrm{u_R}, \mathrm{c_R}, \mathrm{t_R}$	$+\frac{2}{3}$	0	0	$+\frac{4}{3}$
$e_\mathrm{R}, \mu_\mathrm{R}, \tau_\mathrm{R}$	-1	0	0	-2	$\mathrm{d_R}, \mathrm{s_R}, \mathrm{b_R}$	$-\frac{1}{3}$	0	0	$-\frac{2}{3}$

Table 1: The values of weak isospin and hypercharge for each of the fundamental fermions. The L and R subscripts indicate the handedness of the fermion. Right-handed neutrinos ($\nu_{e\mathrm{R}}, \nu_{\mu\mathrm{R}}, \nu_{\tau\mathrm{R}}$) do not exist in the Standard Model, they are included in the table for completeness only.

17.2 Weak Isospin and Hypercharge Currents

Particles with non-zero values of weak isospin couple to a set of W-bosons: W^1, W^2 and W^3 with a coupling strength g_W.

Particles with non-zero values of hypercharge couple to one boson B^0 with a coupling strength $g'_W/2$.

All fermions with non-zero values of weak isospin sit in one of the isospin doublets (equations (17.1), (17.2)). The three W-bosons have an SU(2) symmetry, described by the Pauli matrix structure in the following equations. The interaction of the fermions with the W^1, W^2 and W^3 bosons are:

$$\begin{aligned} j_\mu^{W1} &= (g_W|T_3|)\,\overline{\chi_\mathrm{L}}\gamma^\mu \begin{pmatrix} 0 & 1 \\ 1 & 0 \end{pmatrix} \chi_\mathrm{L} \\ j_\mu^{W2} &= (g_W|T_3|)\,\overline{\chi_\mathrm{L}}\gamma^\mu \begin{pmatrix} 0 & -i \\ i & 0 \end{pmatrix} \chi_\mathrm{L} \\ j_\mu^{W3} &= (g_W|T_3|)\,\overline{\chi_\mathrm{L}}\gamma^\mu \begin{pmatrix} 1 & 0 \\ 0 & -1 \end{pmatrix} \chi_\mathrm{L} \end{aligned} \tag{17.3}$$

where χ_L are any one of the weak isospin doublet in equations (17.1) and (17.2). Here you should think of the components of the χ_L representing the spinors of these particles. Note that the strength of the fermion interaction with the boson is $g_W T_3$.

All fermions (with the exception of right-handed neutrinos, which are not present in the Standard Model) have non-zero hypercharge and therefore interact with the B^0 boson. This boson has a U(1) symmetry. For an example, the interaction of an electron with the B^0 boson is written as:

$$j_\mu^Y = (\frac{1}{2}g'_W\,Y_e)\,\overline{e}\gamma^\mu e = \frac{1}{2}g'_W(Y_{e\mathrm{L}}\,\overline{e_\mathrm{L}}\gamma^\mu e_\mathrm{L} + Y_{e\mathrm{R}}\,\overline{e_\mathrm{R}}\gamma^\mu e_\mathrm{R}) \tag{17.4}$$

where:

- Y_e is the hypercharge of the electron. It is different for the left-handed and right-handed components on the electron, which is why the equation is expanded show the coupling between the left- and right-handed components separately.

- e_{L} is a spinor for the left-handed electron
- e_{R} is a spinor for the right-handed electron

Note the strength of the interaction is $g'_W Y/2$.

17.3 Electroweak Unification

The combined electroweak interaction is written as a sum of all the equations (17.4) and (17.3) above.

The physically observed bosons, W^+, W^-, Z^0 and γ are linear superposition of the W^1, W^2, W^3 and B^0 bosons:

$$\begin{aligned} W^+ &= \frac{1}{\sqrt{2}}(W^1 - iW^2) \qquad & W^- &= \frac{1}{\sqrt{2}}(W^1 + iW^2) \\ Z^0 &= W^3 \cos\theta_W - B^0 \sin\theta_W \qquad & \gamma &= W^3 \sin\theta_W + B^0 \cos\theta_W \end{aligned} \tag{17.5}$$

where the $\cos\theta_W$ and $\sin\theta_W$ terms insure the correct normalisation. θ_W is known as the weak mixing angle.

17.3.1 Charged Current Interactions

The coupling between the W^+ and W^- states is therefore:

$$\frac{1}{\sqrt{2}}(g_W|T_3|) = \frac{1}{2\sqrt{2}} g_W \tag{17.6}$$

Where the $1/\sqrt{2}$ term comes from the normalisation of the $W^\pm$ states. The $(1-\gamma^5)$ term in the W-boson interaction is integrated into the left-handed component, as the left-handed projection operator includes a $(1-\gamma^5)$ term (see section 7.5).

17.3.2 Photon Interactions

The coupling between the electron and the photon is:

$$\begin{aligned} & j_\mu^{W3} \sin\theta_W + j_\mu^Y \cos\theta_W \\ &\quad = (g_W|T_3|\sin\theta_W)\,\overline{\chi_{\mathrm{L}}}\gamma^\mu \begin{pmatrix} 1 & 0 \\ 0 & -1 \end{pmatrix} \chi_{\mathrm{L}} + (\tfrac{1}{2} g'_W Y_e \cos\theta_W)\,\overline{e}\gamma^\mu e \\ &\quad = -(\tfrac{1}{2} g_W \sin\theta_W)\overline{e_{\mathrm{L}}}\gamma^\mu e_{\mathrm{L}} + (\tfrac{1}{2} g'_W \cos\theta_W)(-\overline{e_{\mathrm{L}}}\gamma^\mu e_{\mathrm{L}} - 2\overline{e_{\mathrm{R}}}\gamma^\mu e_{\mathrm{R}}) \\ &\quad = -\tfrac{1}{2}(g_W \sin\theta_W + g'_W \cos\theta_W)(\overline{e_{\mathrm{L}}}\gamma^\mu e_{\mathrm{L}}) - (g'_W \cos\theta_W)(\overline{e_{\mathrm{R}}}\gamma^\mu e_{\mathrm{R}}) \end{aligned}$$

This is consistent with the coupling strength of e between the electron and photon if:

$$e = g'_W \cos\theta_W = g_W \sin\theta_W \tag{17.7}$$

Lepton	c_V	c_A	Quark	c_V	c_A
ν_e, ν_μ, ν_τ	$\frac{1}{2}$	$\frac{1}{2}$	u, c, t	$\frac{1}{2} - \frac{4}{3}\sin^2\theta_W \sim 0.19$	$\frac{1}{2}$
e, μ, τ	$\frac{1}{2} + -2\sin^2\theta_W \sim -0.03$	$-\frac{1}{2}$	d, s, b	$\frac{1}{2} + \frac{2}{3}\sin^2\theta_W \sim -0.34$	$-\frac{1}{2}$

Table 2: Vector and axial vector coupling constants c_V and c_A between fermions and Z-bosons.

Therefore the mixing angle θ_W can be defined as:

$$\sin^2\theta_W = \frac{g_W'^2}{g_W^2 + g_W'^2} (\approx 0.22) \tag{17.8}$$

The value for θ_W is not predicted by the electroweak model, it must be measured experimentally.

17.3.3 Neutral Current Interaction

The Z^0 boson is defined in equation (17.5). The interaction between an electron and the Z boson can be written as the following current:

$$\begin{aligned} j_\mu^z &= \frac{g_W}{\cos\theta_W}\left[(T_3 - Q\sin^2\theta_W)(\overline{e_{\mathrm{L}}}\gamma^\mu e_{\mathrm{L}}) - (Q\sin^2\theta_W)(\overline{e_{\mathrm{R}}}\gamma^\mu e_{\mathrm{R}})\right] \\ &= \frac{g_Z}{2}\,\bar{e}\,\gamma^\mu(c_V^e - c_A^e\gamma^5)\,e \end{aligned} \tag{17.9}$$

where e represents the electron spinor. and in the last line we have written the coupling in terms introduced in section 7.9. We can now identify the following constants:

$$g_Z = \frac{g_W}{\cos\theta_W} \qquad c_V = T_3 - 2Q\sin^2\theta_W \qquad c_A = T_3 \tag{17.10}$$

These constants are shown for the different fermions in table 2.

Note that c_V and c_A have different values for different types of fermion. These couplings are predicted by the electroweak theory, and verified by experimental measurements.

17.4 Summary of the Electroweak Model

In the previous section we have recovered the known behaviour of the weak and electromagnetic bosons: $W^\pm, Z$ and γ.

We did this by introducing an SU(2) symmetry (3 bosons) coupling to weak isospin with a coupling constant g_W and a U(1) symmetry (1 boson) coupling to weak hypercharge with a coupling constant $g_W'/2$. These four bosons are mix together to form the physical W^+, W^-, Z and γ.

Electroweak Theory is often called SU(2) $\times$ U(1) model. All of the properties of electroweak interactions described by:

- the intrinsic charges of the fermions
- the SU(2) $\times$ U(1) symmetry
- the coupling constants g_W and g'_W. g_W and g'_W are free parameters that need to be measured.

17.5 Electroweak Parameters

If electroweak symmetry were exact, the physical bosons would all be massless. To generate the masses of the W and Z bosons, the symmetry is **spontaneously broken**, through the **Higgs mechanism**, which will be discussed in detail in the next section. The mass scale at which the symmetry is broken is known as the **electroweak scale**, $v \approx 246$ GeV.

All of the fundamental parameter of the electroweak model are combinations of g_W, g'_W and v. The values for these can be extracted from three independent parameters. The three most precisely measured quantities are:

- The electric charge, e, measured by the electric dipole moment.
- The Fermi Constant, G_F (precision: 0.9×10^{-5}) measured by the muon lifetime.
- The mass of the Z boson, M_Z (precision: 2.3×10^{-5}).

Some of the electroweak parameters are:

$$e = \frac{g_W\, g'_W}{\sqrt{g_W^2 + g_W'^2}} \qquad M_Z = \frac{1}{2} v \sqrt{g_W^2 + g_W'^2} \qquad G_F = \frac{1}{\sqrt{2}\, v^2} \tag{17.11}$$

$$\sin^2\theta_W = \frac{g_W'^2}{g_W^2 + g_W'^2} \qquad M_W = \frac{v\, g_W}{2} \tag{17.12}$$

The masses of the W and Z bosons are measured to very high precision:

$$M_W = 80.425(38)\text{GeV} \qquad M_Z = 91.1876(21)\text{GeV} \tag{17.13}$$

and the ratio of the masses gives the weak mixing angle:

$$\cos\theta_W = 0.8819 \qquad \sin^2\theta_W = 0.2221 \tag{17.14}$$

17.6 Z^0 Production at LEP

From 1989 to 2001 four experiments, ALEPH, DELPHI, L3 and OPAL, took data at the Large Electron Positron (LEP) collider at CERN. During the first six years detailed measurements of e^+e^- collisions at the Z^0 mass were made. The width of the Z^0 boson is measured to very high precision:

$$\Gamma_Z = 2.4952(23)\text{GeV} \tag{17.15}$$

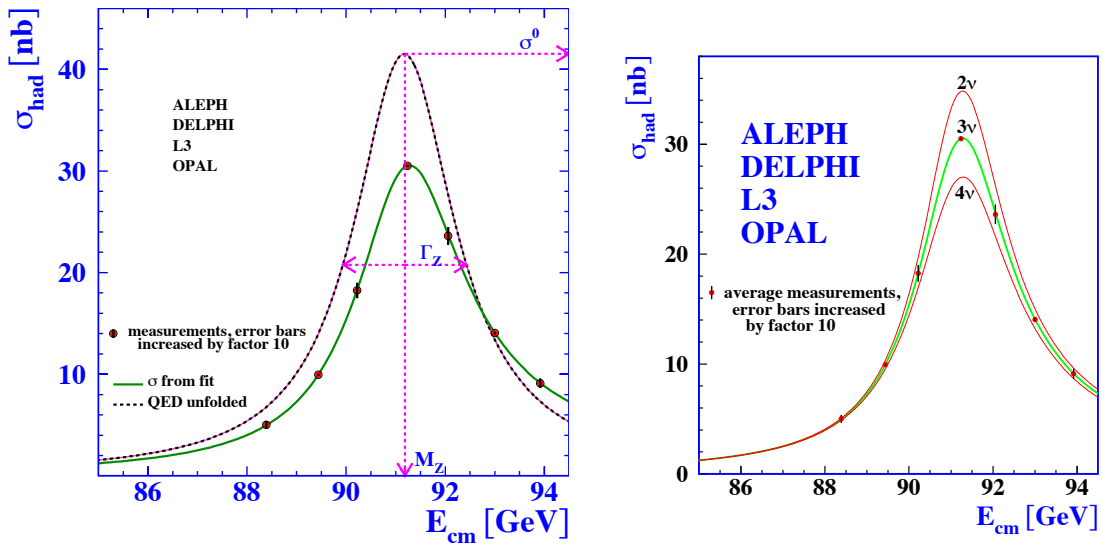

Figure 17.1: Measurements of the $\sigma(e^+e^- \to Z \to \text{hadrons})$ cross section as a function of e^+e^- collision energy from the LEP collider. Note that the error bars are increased by a factor of ten. These measurements are used to extract the mass and width of the Z boson, show that there are only three neutrinos with $m_\nu < m_Z/3$.

and the ratio of the couplings of the Z^0 to hadrons and charged leptons (ℓ) is:

$$R = \frac{\Gamma(Z^0 \to \text{hadrons})}{\Gamma(Z^0 \to \ell^+\ell^-)} = 20.767(25) \tag{17.16}$$

The couplings of the Z^0 to the different fermions are predicted by electroweak theory:

$$\Gamma(Z^0 \to f\bar{f}) = \frac{g^2}{48\pi\cos^2\theta_W}(c_V^2 + c_A^2)M_Z \tag{17.17}$$

$$\Gamma(Z^0 \to \ell^+\ell^-) = 84 \text{ MeV} \qquad \Gamma(Z^0 \to \nu_\ell\bar{\nu}_\ell) = 166 \text{ MeV} \tag{17.18}$$

For the quarks there is an additional colour factor $N_C = 3$, and the $\text{t}\bar{\text{t}}$ decay is not available because of the large top quark mass.

$$\Gamma(Z^0 \to \text{u}\bar{\text{u}}) = \Gamma(Z^0 \to \text{c}\bar{\text{c}}) = 291 \text{ MeV} \tag{17.19}$$

$$\Gamma(Z^0 \to \text{d}\bar{\text{d}}) = \Gamma(Z^0 \to \text{s}\bar{\text{s}}) = \Gamma(Z^0 \to \text{b}\bar{\text{b}}) = 372 \text{ MeV} \tag{17.20}$$

From the total width Γ_Z it is possible to deduce the part due to $Z^0 \to \nu\bar{\nu}$, which is known as the "invisible width", by subtracting the known widths for $Z^0 \to$ hadrons and $Z^0 \to \ell^+\ell^-$. This gives a constraint on the number of types of neutrino with masses $m_\nu < 45$ GeV, $N_\nu = 2.988(23)$, which is consistent with the Standard Model expectation of 3.

The lepton universality of the Z^0 couplings has also been checked to high precision at LEP.

17.7 W Boson Production at Colliders

The W and Z bosons were originally discovered at CERN in proton-antiproton collisions, where they are produced by quark-antiquark annihilation, e.g. $u\bar{d} \to W^+$. The W was first measured using $W \to \ell\nu_\ell$, where ℓ is an electron or muon and the neutrino is inferred from transverse missing energy. The W can also be reconstructed from its decays to quarks.

Precise measurements of the W boson mass and width have been made in proton-antiproton collisions at the Tevatron collider and in $e^+e^- \to W^+W^-$ production at the LEP collider:

$$M_W = 80.395(15)\ \text{GeV} \qquad \Gamma_W = 2.085(42)\ \text{GeV} \tag{17.21}$$

17.8 Precision Tests of Electroweak Theory*

These are summarised at `http://lepewwg.web.cern.ch` and for the Tevatron at `http://tevewwg.fnal.gov`.

The plot shows the number of σ by which each measurement deviates from the electroweak theory prediction. Overall the agreement is very good, but the A_{FB} measurement shows a 3σ discrepancy.

	Measurement	Fit
$\Delta\alpha^{(5)}_{had}(m_Z)$	0.02750 ± 0.00033	0.02759
m_Z [GeV]	91.1875 ± 0.0021	91.1874
Γ_Z [GeV]	2.4952 ± 0.0023	2.4959
σ^0_{had} [nb]	41.540 ± 0.037	41.478
R_l	20.767 ± 0.025	20.742
$A^{0,l}_{fb}$	0.01714 ± 0.00095	0.01645
$A_l(P_\tau)$	0.1465 ± 0.0032	0.1481
R_b	0.21629 ± 0.00066	0.21579
R_c	0.1721 ± 0.0030	0.1723
$A^{0,b}_{fb}$	0.0992 ± 0.0016	0.1038
$A^{0,c}_{fb}$	0.0707 ± 0.0035	0.0742
A_b	0.923 ± 0.020	0.935
A_c	0.670 ± 0.027	0.668
A_l(SLD)	0.1513 ± 0.0021	0.1481
$\sin^2\theta^{lept}_{eff}(Q_{fb})$	0.2324 ± 0.0012	0.2314
m_W [GeV]	80.385 ± 0.015	80.377
Γ_W [GeV]	2.085 ± 0.042	2.092
m_t [GeV]	173.20 ± 0.90	173.26

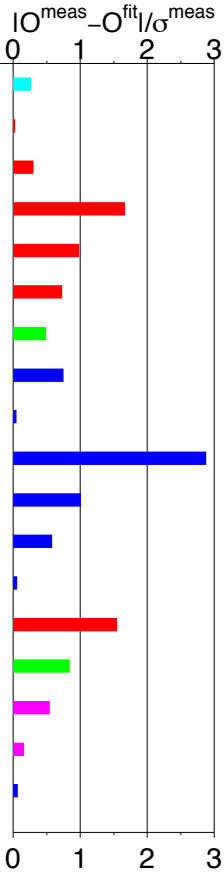

March 2012

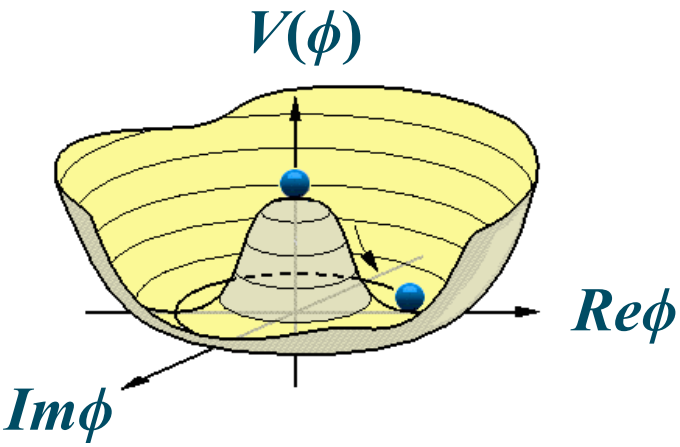

Figure 18.1: The Higgs potential.

18 The Higgs Boson

18.1 Spontaneous Symmetry Breaking

If the ground state configuration of a system does not display the full symmetry that might be expected from the Hamiltonian, it is said to be "spontaneously broken", and the symmetry is said to be "hidden". An example is a set of table napkins placed between people at a dining table. The first person who picks up a napkin, either with their left or right hand, breaks the symmetry, and all the other people have to follow with the same hand.

An example from a physical system is ferromagnetism. Below the critical temperature T_C, all the spins of the atoms align, but the direction of alignment is arbitrary, i.e. all alignments have equal energy. During the phase transition, in the absence of an external magnetic field, the rotational symmetry is spontaneously broken, and an arbitrary direction of magnetization is chosen. If there is an external magnetic field this breaks the symmetry explicitly and aligns the spins along the field direction.

18.2 The Higgs Field

To explain the non-zero masses of the weak vector bosons, we introduce a spontaneous breaking of the electroweak symmetry between the γ, W, Z bosons. We assign a **vacuum expectation value**, v, to a **Higgs field**, $\langle\phi\rangle$. The Higgs potential energy distribution a "Mexican hat" shape, shown in figure 18.1:

$$V(\phi) = -\mu^2\phi^\dagger\phi + \lambda(\phi^\dagger\phi)^2 \qquad \mu^2 > 0 \quad \lambda > 0 \tag{18.1}$$

$V(\phi)$ is minimised around a circle in the complex plane defined as:

$$\langle\phi\rangle = -v \qquad v = \sqrt{\frac{\mu^2}{2\lambda}} \tag{18.2}$$

v is known as the vacuum expectation value, and is measured to be $v = 246$ GeV. Note that the Higgs field exists in a vacuum, i.e. independent of the presence of matter.

The simplest form of the Higgs field is described by one doublet of weak isospin with four parameters:

$$\phi = \begin{pmatrix} \phi^+ \\ \phi^0 \end{pmatrix} = \frac{1}{\sqrt{2}} \begin{pmatrix} \phi_1 + i\phi_2 \\ \phi_3 + i\phi_4 \end{pmatrix} \tag{18.3}$$

The + and 0 indicate the value of the electric charge (+1 or neutral). Note that there are more complicated forms of the Higgs field beyond the Standard Model, which will be discussed in the next lecture.

18.3 The Standard Model Higgs Boson

When electroweak symmetry is spontaneously broken, three of ϕ_i degrees of freedom are used to give mass to W^+, W^- and Z^0 bosons. This fixes three of the degrees of ϕ_i freedom: two charged and one neutral.

The value of ϕ for the for ground state (ϕ_0) can then be written in terms of the remaining free parameter:

$$\phi_0 = \frac{1}{\sqrt{2}} \begin{pmatrix} 0 \\ v \end{pmatrix} \tag{18.4}$$

Where $v = \sqrt{\mu^2/2\lambda}$ (equation (18.2)).

An excitation (fluctuations) of the Higgs field will be around this minimum and can be written as:

$$\phi(x) = \phi_0 + h(x) = \begin{pmatrix} 0 \\ v + h(x) \end{pmatrix} \tag{18.5}$$

Substituting $\phi(x) = \frac{1}{\sqrt{2}}(v + h(x))$ into equation (18.1) and expanding to second order in $h(x)$ gives:

$$V(\phi) = -\mu^2 \left(\frac{v + h(x)}{\sqrt{2}}\right)^2 + \lambda \left(\frac{v + h(x)}{\sqrt{2}}\right)^4 = V(\phi_0) + \lambda v^2 h^2 + \mathcal{O}(h(x)^3) \tag{18.6}$$

In quantum field theory a term quadratic in the field describes a particles mass. The term $\lambda v^2 h^2$ therefore describes a physical particle $h(x)$ with a mass $m_H^2/2 = \lambda v^2$, or $m_H = \sqrt{2\lambda}\, v$.

This fluctuation around the minimum of the potential describes a spin-0 particle with a mass $m_H = \sqrt{2\lambda}\, v$ which we call the Higgs boson! It is electrically neutral and has zero spin. Its mass is unknown but can be constrained by experiment and by electroweak theory.

18.4 Higgs Couplings to Gauge Bosons

The Higgs field also interacts with the electroweak currents and adds additional terms to the electroweak Lagrangian of:

$$g_W^2 \frac{v^2}{4} W^+ W^- + (g_W^2 + g_W'^2) \frac{v^2}{8} Z^0 Z^0 \tag{18.7}$$

where the g_W and g'_W terms are the couplings between vector bosons and the Higgs field. From this we can identify the W and Z boson masses:

$$M_W = \frac{v g_W}{2} \qquad M_Z = \frac{v\sqrt{g_W^2 + g_W'^2}}{2} \tag{18.8}$$

The vacuum expectation value of the Higgs field, v, determines the mass scale of the weak vector bosons. The measured masses give the **electroweak scale** parameter:

$$v = \frac{2 M_W \sin\theta_W}{e} = 246 \text{ GeV} \tag{18.9}$$

Note that v is a free parameter of the electroweak theory, determined from experimental measurements.

The photon does not acquire a mass as a result of the Higgs mechanism. Note that the Standard Model Higgs boson has no charge, so does not couple to the photon.

18.5 Higgs couplings to Fermions

The Lagrangian acquires additional terms for each fermion type f:

$$g_f(\bar{f} f) v = g_f(\bar{f}_{\mathrm{L}} f_{\mathrm{R}} + \bar{f}_{\mathrm{R}} f_{\mathrm{L}}) v \tag{18.10}$$

The Higgs couples the fermions to v, a parameter with a mass dimension. The fermion masses are proportional to the couplings of the fermions to the Higgs field g_f, which are still free parameters in the Standard Model.

We interpret $g_f v$ as the mass of the fermion. Therefore we say The Higgs mechanism explains the masses of all the quarks and charged leptons!

Note that the coupling of the fermions to the Higgs boson is proportional to the g_f, or equivalently to the fermion mass.

18.6 Decays of the Higgs Boson

The strength of Higgs boson couplings in order is:

- W-boson
- Z-boson

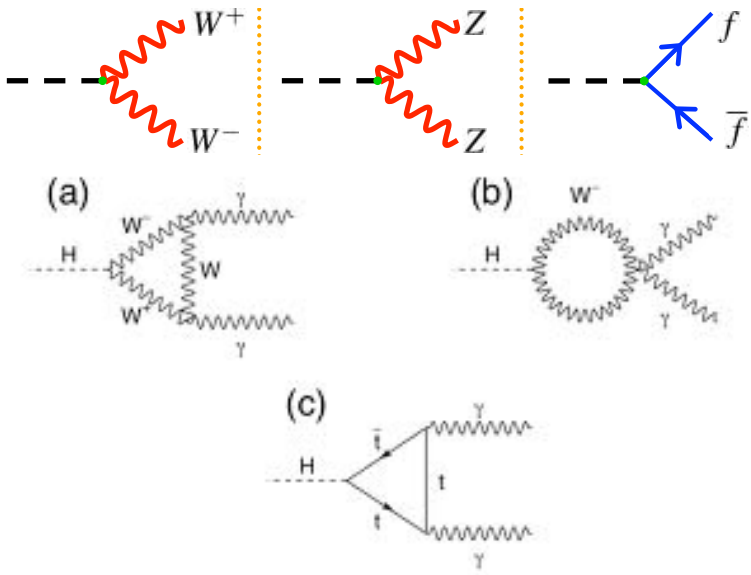

Figure 18.2: Feynman diagrams illustrating Higgs bosons decays. Here, f represents any fermion.

- fermions: from heaviest to lightest

The Higgs can also couple to pairs of photons through loop diagrams. The relevant Feynman diagrams are shown in figure 18.2.

The actual decay modes of the Higgs boson depend on its mass. The predicted branching ratios are illustrated in figure 18.3. The main constraint is whether there is if Higgs has enough mass to decay to two W-bosons (W-bosons being the Higgs preferred decay mode as it couples to W-boson most strongly). The decay modes are:

- $M_H < 2M_W$: the main decay is $H^0 \to b\bar{b}$, but the rare decays $H^0 \to \tau^+\tau^-$ and $H^0 \to \gamma\gamma$ may also be observable.

- $M_H > 2M_Z$: the main decays are $H^0 \to W^+W^-$ and $H^0 \to Z^0Z^0$, The decay of two Z^0 bosons to four leptons is a particularly clean signature.

- $M_H > 650$ GeV: for very large Higgs masses the decay width Γ_H is large, and the production cross-section is small even at the LHC. In this range it will be hard to observe a mass peak.

18.7 First Searches for the Higgs Boson

During the 1990's the LEP collider at CERN (introduced in section 17.6) searched for the Higgs boson through $e^+e^- \to ZH$ production.

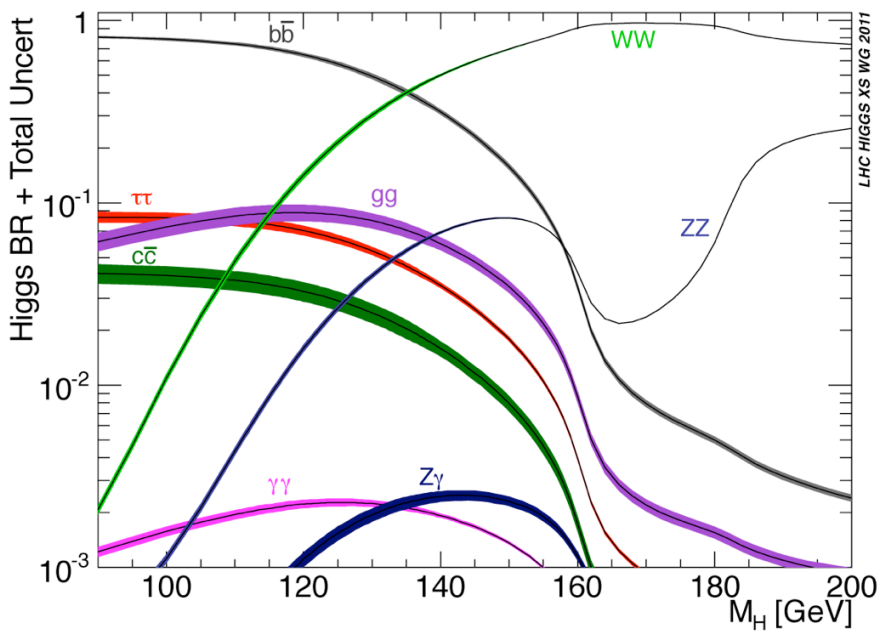

Figure 18.3: Branching ratios for Higgs decays as a function of Higgs mass.

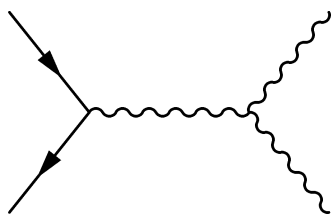

The measurements were sensitive to values of m_H up to $\sqrt{s} - m_Z$, where $\sqrt{s}$ is the centre of mass energy of the collider. LEP did not observe any conclusive evidence for the Higgs boson and therefore set a limit of $m_H > 144.4$ GeV.

18.8 Electroweak Constraints on the Higgs Mass

Diagrams involving Higgs boson couplings enter as corrections to all Standard Model predictions for electroweak processes:

- The determination of $\sin^2\theta_W$ from neutrino scattering.
- The measurements of the masses and widths of the W and Z bosons.
- Polarization asymmetries in lepton pair production $e^+e^- \to \ell^+\ell^-$.

These can be used to provide indirect constraints on the Higgs boson mass. These are illustrated in figure 18.4.

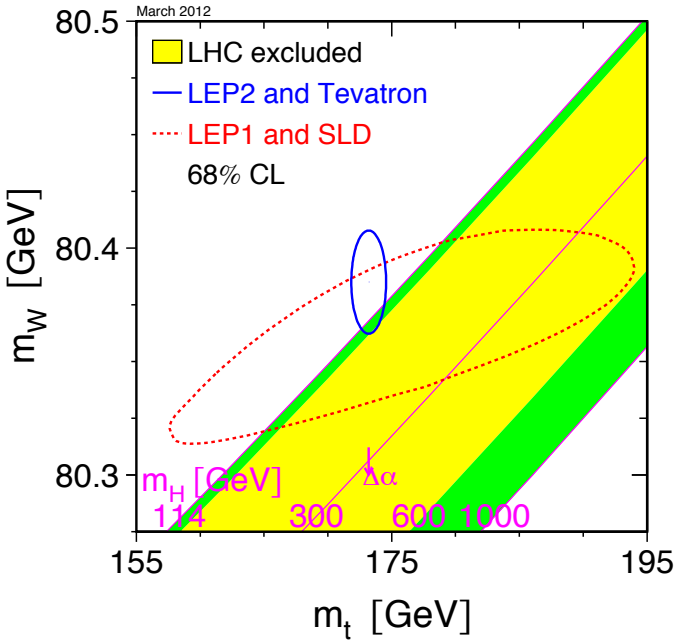

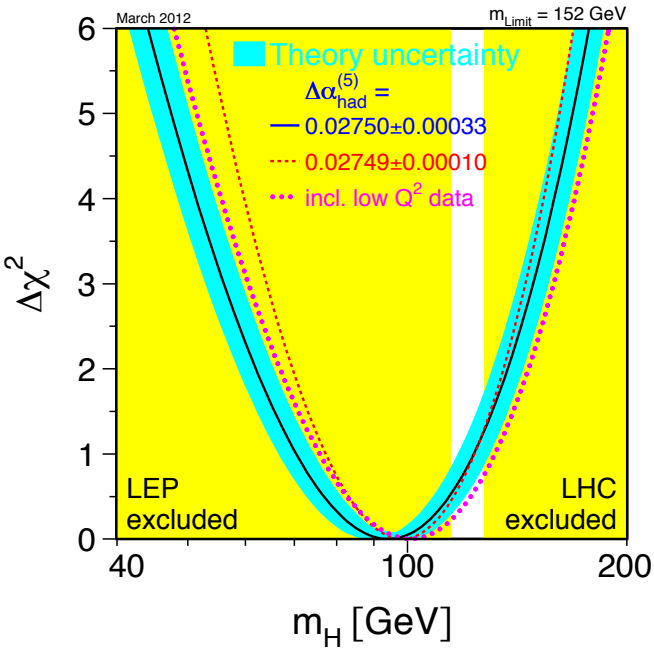

Figure 18.4: Top - the sensitivity of the Higgs mass to the mass of the top quark and the mass of the W boson. Bottom - constraints on the Higgs mass. The parabolic curves come from the electroweak constraints. The excluded region to the left is the result of the direct experimental searches at LEP, the excluded region to the right is from searches at the LHC and the Tevatron.

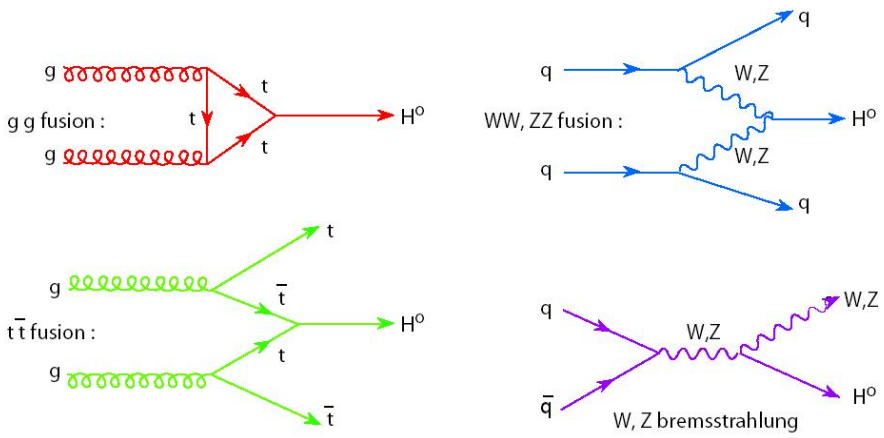

Figure 18.5: Feynman diagrams for Higgs production processes at hadron colliders.

18.9 Production of the Higgs at Hadron Colliders

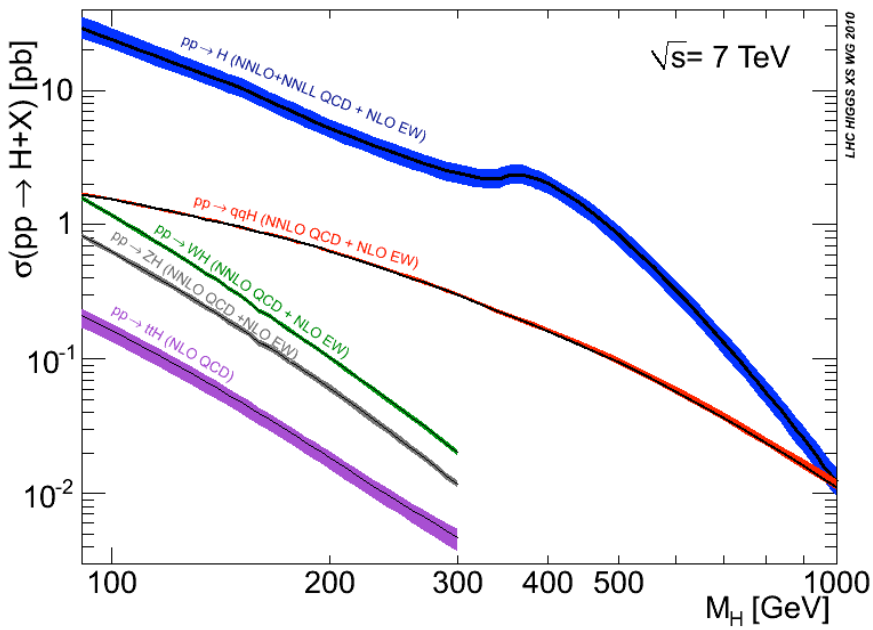

Figure 18.6: Predicted cross-sections for Higgs production processes at the LHC, as a function of the Higgs boson mass, m_H.

The search for the Higgs boson is now continuing at the Large Hadron Collider at CERN. The LHC began taking data in 2010 with $\sqrt{s} = 7$ TeV. In December 2011 the first results were announced ruling out a wide range of masses for the value of the Standard Model Higgs boson mass. These are illustrated in figure 18.7. Final results from the Tevatron proton-antiproton collider with $\sqrt{s} = 1.96$ TeV have also been announced recently.

The main Higgs production mechanisms at a hadron collider are shown in figure 18.5

and 18.6:

- Direct production through gluon-gluon fusion and an intermediate top quark loop. This is the dominant process.
- Associated production with top quarks.
- Fusion of either $W^{\pm}$ or Z^0 bosons.
- Associated production with either a Z^0 or W boson.

The fusion processes have large cross-sections but are hard to identify experimentally. The associated production processes have small cross-sections but clear signatures.

The overall results from LEP, the Tevatron and the LHC rule out the following masses for the Higgs boson: $m_H \lesssim 120$ GeV and 130 GeV $\lesssim m_H \lesssim 600$ GeV.

The Tevatron and the LHC experiments (ATLAS and CMS) all observe an excess in Higgs-like events (compared to what would be expected if there were no Higgs-like events) for $m_H \sim 125$ GeV. This is illustrated as the bump above the yellow band at $m_H \sim 125$ GeV in figure 18.7. However, there are currently not enough statistics to confirm if this observed excess is actually due to Higgs bosons being produced. The LHC will continue to take data in 2012, hopefully this will be enough to confirm or dismiss this effect!

(See the lecture slides for slides from ATLAS and CMS presented at recent conferences about these exciting results!)

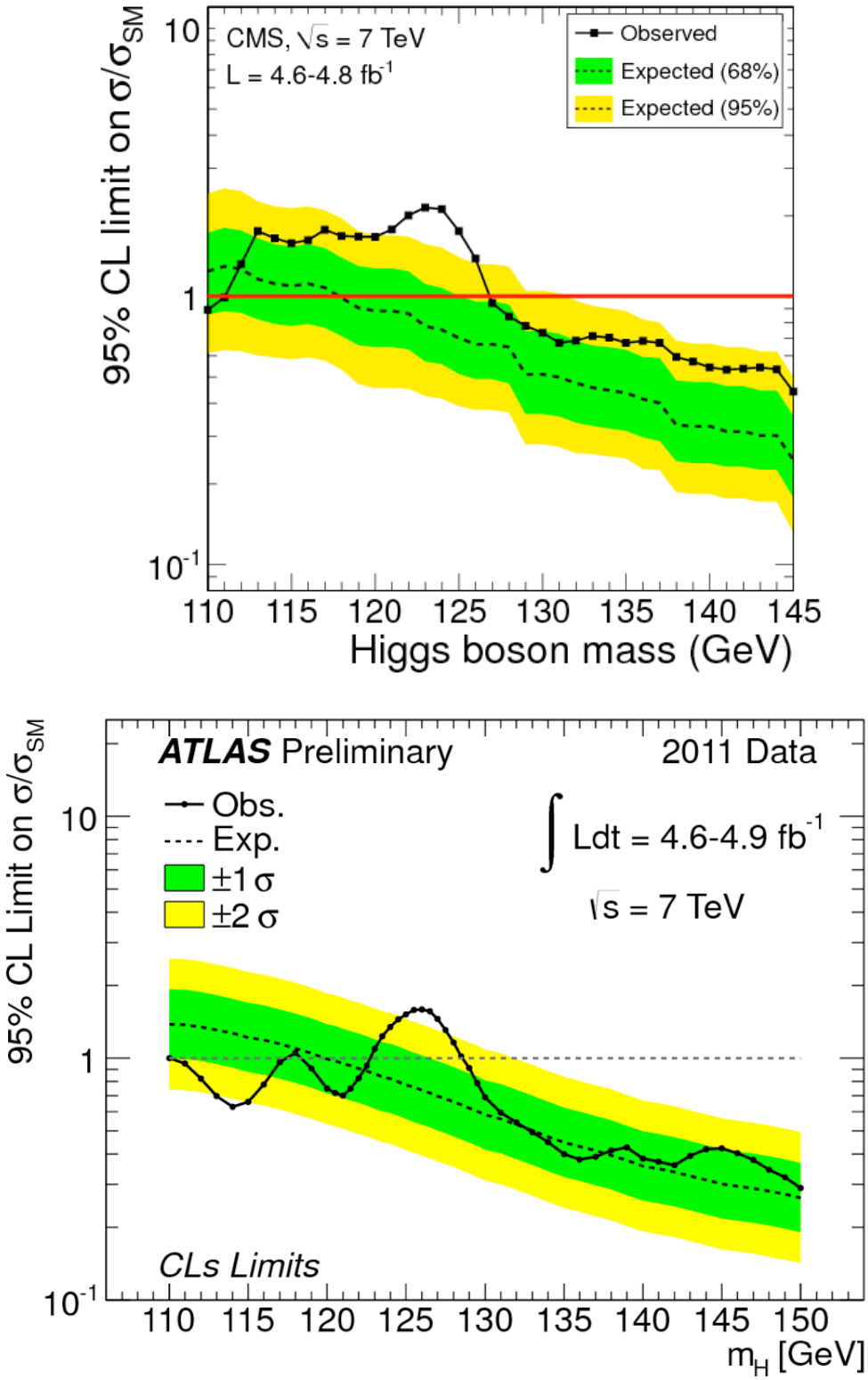

Figure 18.7: Limits on the Higgs boson mass from the ATLAS experiment at the LHC. The Higgs boson mass is now constrained to be between ~ 120 and 127 GeV, or $m_H >\sim 550$ GeV. The bump at $m_H \sim 125$ GeV could be the first sign of Higgs boson production! (However it is not yet significant to say for sure if this is really the Higgs boson.)

19 Beyond the Standard Model

There are many experimental motivations for believing that the Standard Model of particle physics is incomplete, including:

- Neutrino oscillations are not explained.
- The matter-antimatter asymmetry of the universe requires baryon number violation, and a much larger source of CP violation than is provided by the CKM matrix.
- There is no candidate for dark matter (20% of the universe).

There are a large number of different models that have been proposed to go beyond the Standard Model. In most cases these models predict new particles and couplings at or just above the electroweak scale. An exception to this is "string" theory, which deals with phenomena near the Planck scale which are unlikely to be testable in the foreseeable future.

19.1 Multiple Higgs doublets

One of the simplest extension to the Standard Model is a two Higgs doublet model, in which one Higgs doublet couples to the d-type quarks and the charged leptons, and the other doublet couples to the u-type quarks. Note that electroweak symmetry breaking requires the Higgs to be doublets of SU(2) weak isospin, but does not restrict the number of doublets. There are two vacuum expectation values v_d and v_u which satisfy $v_d^2 + v_u^2 = v^2$, where $v = 246$ GeV. The ratio $v_u/v_d = \tan\beta$ is a free parameter. An advantage of two Higgs doublet models is that they naturally suppress flavour-changing neutral currents associated with Higgs boson exchange.

In a two Higgs doublet model there are eight independent ϕ parameters of which only three get "eaten" during electroweak symmetry breaking, so there are five corresponding Higgs bosons, the $H^\pm$, h^0, H^0 and A^0. The lightest h^0 is similar to the Standard Model Higgs, but the charged Higgs in particular has distinctive signatures and decay modes, e.g. $H^+ \to t\bar{b}$.

19.2 Supersymmetry (SUSY)

SUSY models introduce an explicit symmetry between fermions and boson. For each Standard Model fermion there is a spin 0 supersymmetric partner. They are known as **squarks** (stop, sbottom ...), and **sleptons** (selectron, smuon, sneutrino ...), and are notated $\tilde{q}$ and $\tilde{\ell}$.

Similarly for every Standard Model boson there is a spin 1/2 partner. They are known as **neutralinos** (photino, Zino or Bino, gluino, higgsino), $\tilde{\chi}^0$, and **charginos** (Wino), $\tilde{\chi}^+$.

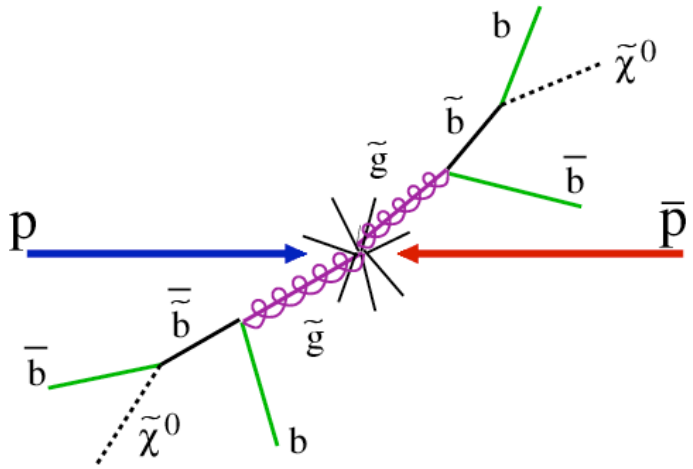

Figure 19.1: A potential SUSY particle production mechanism at the LHC.

19.3 Grand Unification

The electromagnetic and weak interactions were unified at the electroweak scale. By analogy it is hoped that the strong and electroweak interactions can be unified at some higher mass scale. An extrapolation of the running coupling constant α_s suggests a unification scale $M_X \approx 10^{15}$ GeV.

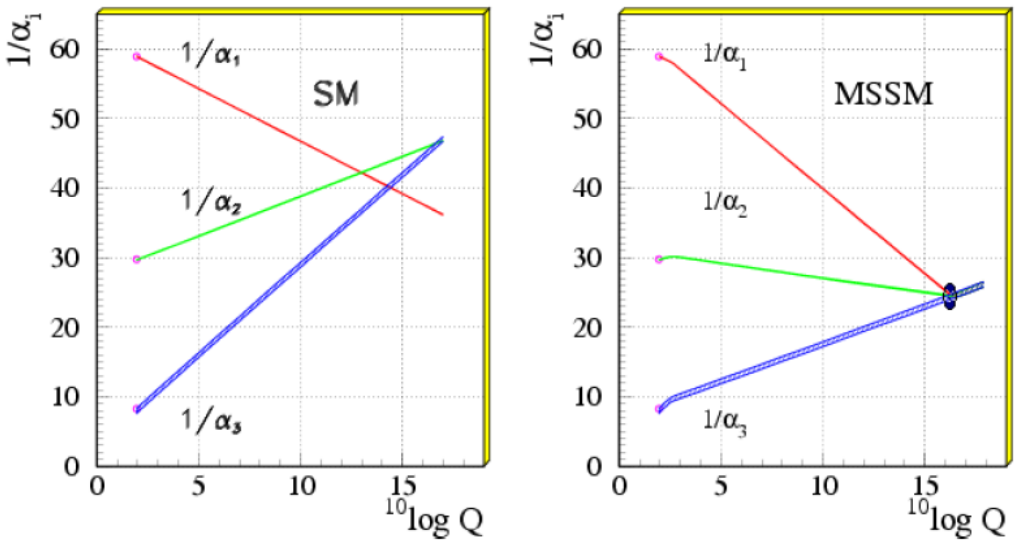

Figure 19.2: Evolution of coupling constants from the electroweak to the GUT scale in the Standard Model and the MSSM.

19.4 Extra Dimensions

String theories require extra dimensions (typically 10 or 11 in total), which are said to be "compactified" over small distances corresponding to high mass scales. These dimensions are either "universal" or anomalous ("warped" or Randall-Sundrum). Within the extra dimensions there can be excitations of Kaluza-Klein graviton states. The search for these states is similar to the search for the Z' and gives limits of ≈ 1 TeV.